International Journal of Applied Science and Engineering Review

IJASER

ISSN: 2582-6271

Vol. 7, Issue. 6, Nov-Dec 2026, page no. 31-42

To cite this article: Hanif Farrel Ardan, Agnes Theresia Petra S and Hargono Hargono (2026). ETHANOL DEHYDRATION VIA ADSORPTION USING COMPOUND STARCH ADSORBENT (CSA), International Journal of Applied Science and Engineering Review (IJASER) 7 (6): 31-42 Article No. 306 Sub Id 442

ETHANOL DEHYDRATION VIA ADSORPTION USING COMPOUND STARCH ADSORBENT (CSA)

Hanif Farrel Ardan[1]*, Agnes Theresia Petra S[2] and Hargono Hargono[3]

[(1,2,3)]Diponegoro University, Department of Chemical Engineering, Faculty of Engineering, Universitas Diponegoro, Semarang 50275, Indonesia
el.farrel1010@gmail.com Corresponding author: hargono@che.undip.ac.id

DOI: https://doi.org/10.52267/IJASER.2026.7603

ABSTRACT

Ethanol is an important compound widely used as an alternative fuel, solvent, and feedstock in the chemical industry. However, conventional distillation can only produce ethanol with a purity of approximately 95–96% due to the formation of an ethanol-water azeotrope, necessitating further purification to obtain dehydrated ethanol. This study aimed to synthesize and characterize a Compound Starch Adsorbent (CSA) derived from cassava and corn starch and to evaluate the effects of initial ethanol concentration and pellet size on the dehydration process. FTIR characterization confirmed the presence of active hydroxyl (–OH) groups at 3370.59 cm^{-1}, which serve as effective water adsorption sites. The distillation-adsorption process was conducted using initial ethanol concentrations ranging from 70% to 90% (v/v). The results showed that increasing the feed ethanol concentration led to higher final ethanol purity due to the reduced amount of water requiring adsorption. Pellets with dimensions of 10 × 20 mm exhibited higher adsorption efficiency than 20 × 30 mm pellets because of shorter intraparticle diffusion pathways and reduced channeling within the packed bed. Optimum operating conditions were obtained at 85°C, a feed ethanol concentration of 90% (v/v), and a pellet size of 10 × 20 mm, producing ethanol with a final purity of 99.1% (v/v). Increasing the operating temperature to 90–95°C reduced ethanol purity due to enhanced water desorption associated with the exothermic nature of the adsorption process.

KEYWORDS: Ethanol, Compound Starch Adsorbent, Adsorption, Ethanol Dehydration, High-Purity Ethanol

International Journal of Applied Science and Engineering Review

IJASER

ISSN: 2582-6271

Vol. 7, Issue.6, Nov-Dec 2026, page no. 31-42

1. INTRODUCTION

Energy consumption is a key indicator of economic progress and industrial development, serving as a catalyst for growth in both developed and developing countries [1]. The increasing demand for energy driven by industrial expansion and transportation activities has accelerated the depletion of fossil fuel reserves and contributed to serious environmental issues, particularly global warming. Ethanol has emerged as a promising alternative fuel capable of reducing harmful emissions, with significant potential for development in Indonesia due to the abundance of renewable feedstocks. However, conventional distillation is only capable of producing ethanol up to its azeotropic concentration of approximately 95–96% (v/v), which restricts further separation by simple distillation [2]. Therefore, breaking this azeotropic barrier is essential to produce high-purity ethanol for various industrial applications, including chemical synthesis, solvents, and biofuels.

Various dehydration and purification technologies have been developed to overcome this limitation, including distillation, membrane separation, and adsorption. Membrane technology has been widely implemented on a commercial scale [3], while adsorption has attracted considerable attention as a simple, flexible, and cost-effective alternative that enables the utilization of locally available materials. The effectiveness of adsorption largely depends on the characteristics of the adsorbent material employed. Common adsorbents include zeolites [4], activated carbon [5], silica gel, and aerogels, all of which possess high surface areas and porous structures that facilitate water removal from ethanol streams [6].

The availability of high-purity ethanol is essential for supporting the transition toward clean and sustainable energy systems while meeting industrial quality standards. Therefore, one of the major challenges is developing a purification method that is effective, economical, and suitable for practical implementation. In this context, the present study focuses on ethanol dehydration through adsorption using a Compound Starch Adsorbent (CSA) derived from locally available starch sources, namely cassava and corn flour. This approach is expected to produce high-purity ethanol at a relatively low cost while promoting the utilization of renewable agricultural resources, making it applicable not only to large-scale industries but also to small and medium-sized enterprises (SMEs) in Indonesia.

2. MATERIALS AND METHODS

2.1 Materials

The primary materials used in this study consisted of corn flour, serving as the mechanical backbone of the adsorbent, cassava flour as the pore-forming agent, 0.10 M sulfuric acid (H_2SO_4), sodium bicarbonate ($NaHCO_3$), distilled water, and technical-grade ethanol with concentrations of 70%, 75%, 80%, 85%, and 90% (v/v). The experimental setup comprised an adsorption-distillation unit consisting of an electric heating stove, boiler tank, adsorption column (4.8 cm in diameter and 64.5 cm in height, with a packed-

ISSN: 2582-6271

Vol. 7, Issue.6, Nov-Dec 2026, page no. 31-42

bed height of approximately 40 cm containing 374 g of adsorbent), cooling-water reservoir, beaker glass, cooling-water circulation tank, water pump, thermometer, and supporting structures.

2.2 Methods

CSA Synthesis and Characterization

Cassava flour (13.33 g) was dispersed in 320 mL of boiling water and stirred until a homogeneous mixture was obtained. Subsequently, 10.67 mL of 0.10 M H_2SO_4 was added to promote partial acid hydrolysis. Corn flour (200 g) was then gradually incorporated into the mixture until a thick paste was formed. To generate pore structures within the adsorbent matrix, 1.33 g of sodium bicarbonate ($NaHCO_3$) was added as a foaming agent, producing CO_2 gas during the reaction. The resulting paste was molded into cylindrical pellets with two different geometries, namely 10 × 20 mm and 20 × 30 mm, and subsequently dried in an oven at 70°C for at least 7 h. Functional group characterization was conducted using Fourier Transform Infrared Spectroscopy (FTIR).

Adsorption Process

Ethanol dehydration experiments were carried out using an integrated distillation-adsorption system. A fixed volume of 250 mL technical-grade ethanol solution was prepared at initial concentrations of 70%, 75%, 80%, 85%, and 90% (v/v). A total of 374 g of CSA adsorbent pellets with cylindrical dimensions of 10 × 20 mm and 20 × 30 mm were packed into the adsorption column, forming a bed height of approximately 40 cm.

The boiler heater and column thermostat were operated at predetermined temperatures of 85°C, 90°C, and 95°C. The purification process was conducted for 120 min, allowing the entire ethanol-water vapor stream to pass through the fixed-bed adsorbent column. During this stage, water vapor was selectively adsorbed by the active sites present on the starch-based pellets. The purified ethanol vapor exiting the top of the column was subsequently condensed using a water-cooled spiral condenser, and the resulting distillate was collected in a tightly sealed container to minimize ethanol losses caused by re-evaporation into the surrounding environment.

Final Ethanol Concentration Analysis

The concentration of ethanol in the product stream was determined using the pycnometric method based on liquid density measurements. Initially, the empty pycnometer was weighed (m empty). The distillate sample was then introduced into the pycnometer until completely filled and free of air bubbles, after which the filled pycnometer was weighed (m filled). The density of the distillate was calculated using the following equation:

International Journal of Applied Science and Engineering Review

IJASER

ISSN: 2582-6271

Vol. 7, Issue.6, Nov-Dec 2026, page no. 31-42

where ρ is the density of the distillate (g mL^{-1}), mfilled is the mass of the pycnometer containing the sample (g), mempty is the mass of the empty pycnometer (g), and V is the pycnometer volume (mL). The final ethanol concentration (% v/v or % w/w) was subsequently determined by comparing the measured density with standard ethanol density values using Equation (2).

$$C \text{ ethanol} = f(\rho) \quad (2)$$

where Cethanol represents the ethanol concentration and f(ρ) denotes the conversion based on standard ethanol density data.

Adsorption Efficiency Analysis

The effectiveness of the dehydration process was evaluated through adsorption efficiency, which quantifies the increase in ethanol concentration achieved after treatment. Adsorption efficiency (η)(\eta)(η) was calculated using the following equation:

$$5 = \frac{Cf - C}{Ci} \times 100\% \quad (3)$$

where Ci is the initial ethanol concentration (%), and Cf is the final ethanol concentration (%) after the adsorption process.

Gas Chromatography (GC) Analysis

To validate the purity of the final product with high accuracy and to identify possible impurities, the best-performing ethanol sample was analyzed using Gas Chromatography (GC) equipped with a Flame Ionization Detector (FID) at the Integrated Laboratory Unit of Universitas Sebelas Maret (UNS). Absolute ethanol was employed as the reference standard for retention time comparison. The obtained chromatograms were analyzed based on peak retention time and peak area percentage to confirm ethanol purity and evaluate the presence of residual contaminants. This analysis provided an independent verification of the ethanol concentration determined by the pycnometric method and ensured the reliability of the dehydration performance results.

3. RESULTS AND DISCUSSION

3.1 Characterization of Compound Starch Adsorbent (CSA)

Functional Group Analysis via Fourier Transform Infrared Spectroscopy (FTIR)

Functional group characterization of the synthesized CSA adsorbent was carried out using Fourier Transform Infrared Spectroscopy (FTIR) to identify chemical bonds and active functional groups

International Journal of Applied Science and Engineering Review

IJASER

ISSN: 2582-6271

Vol. 7, Issue.6, Nov-Dec 2026, page no. 31-42

responsible for water adsorption during bioethanol dehydration. The resulting FTIR spectrum of the CSA adsorbent is illustrated in Figure 1.

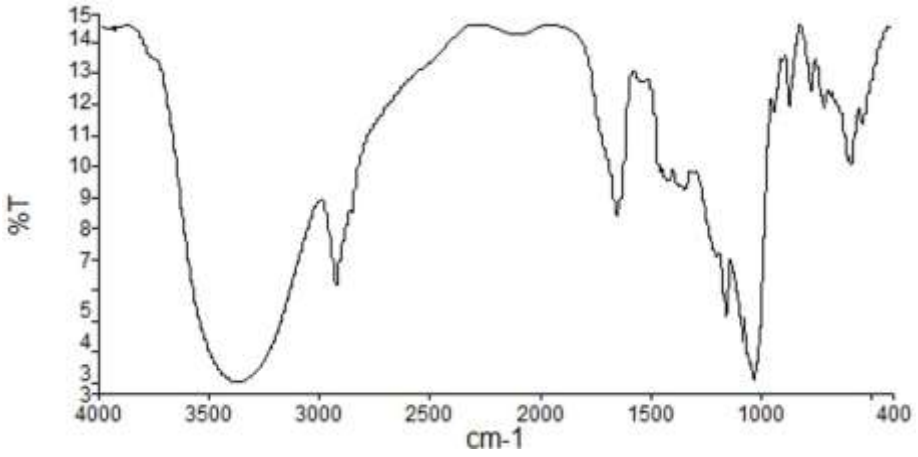

Figure 1: FTIR Spectrum Analysis of CSA Adsorbent

FTIR analysis reveals a broad and intense absorption band at 3370.59 cm^{-1}, corresponding to hydroxyl (−OH) stretching vibrations from cassava and corn starch, as well as bound water molecules. The extensive hydrogen bonding between polysaccharide chains increases the density of active adsorption sites. The peak at 2928.96 cm^{-1} confirms C−H stretching vibrations characteristic of carbohydrate backbone (−CH_2− and −CH−), indicating that the core starch structure remains intact following chemical modification.

The band at 1651.36 cm^{-1}, situated in the overlap region between O−H bending and C−O vibrations, suggests partial acid hydrolysis by H_2SO_4, which induces disruption of the amorphous starch domains and promotes the opening of granular structures. This structural modification is beneficial for adsorption applications because it increases the accessibility of internal hydroxyl groups and enlarges the effective surface area available for moisture adsorption. The presence of this band therefore indicates that chemical treatment altered the starch morphology without causing significant degradation of the primary polysaccharide framework.

In the fingerprint region (1154−1022 cm^{-1}), three prominent absorption peaks are observed at 1154.45 cm^{-1}, 1077.76 cm^{-1}, and 1022.88 cm^{-1}. The peak at 1154.45 cm^{-1} corresponds to asymmetric stretching of glycosidic C−O−C linkages, while the band at 1077.76 cm^{-1} is associated with C−O stretching within the pyranose ring structure. Meanwhile, the intense band at 1022.88 cm^{-1} represents symmetric C−O−C stretching vibrations. These characteristic carbohydrate absorption bands confirm that the starch polymer

ISSN: 2582-6271

Vol. 7, Issue.6, Nov-Dec 2026, page no. 31-42

backbone remains structurally intact after chemical modification. Preservation of the glycosidic network is important because it ensures mechanical stability of the adsorbent while maintaining the abundance of hydrophilic functional groups required for water adsorption.

Additional absorption bands detected between 600 and 708 cm^{-1} may be attributed to residual sulfate or sulfonate species originating from H_2SO_4 treatment. The appearance of these bands suggests the possibility of sulfate ester formation through interactions between sulfuric acid and starch hydroxyl groups. Such surface functionalities can contribute to modifications in surface polarity and may further improve the affinity of the adsorbent toward polar molecules such as water vapor.

The observed absorption characteristics are consistent with previously reported FTIR spectra of cassava-corn starch composites and related starch-based materials [1]. Similar spectral features have been reported for hydroxyl stretching, aliphatic C−H vibrations, and polysaccharide fingerprint regions, indicating that the present CSA adsorbent retains the fundamental chemical characteristics of native starch while undergoing controlled structural modification. The broad absorption band within the 3400−3200 cm^{-1} region corresponds to O−H stretching vibrations arising from hydroxyl groups and hydrogen-bonded water molecules, whereas bands between 3000 and 2800 cm^{-1} are assigned to aliphatic C−H stretching vibrations associated with the carbohydrate backbone [2].

Furthermore, absorption peaks reported at approximately 1743.65 cm^{-1}, 1643.35 cm^{-1}, and 1544.98 cm^{-1} are attributed to amide I and amide II vibrations, representing residual protein and lipid fractions naturally present in starch-derived materials [1]. The amide I band around 1650 cm^{-1} originates primarily from C=O stretching vibrations, while the amide II band near 1540 cm^{-1} is associated with N−H bending and C−N stretching modes. The persistence of these bands indicates that minor proteinaceous components remain detectable after chemical treatment, suggesting that the modification process preserves the overall biochemical integrity of the composite material [3].

Overall, the FTIR analysis demonstrates that H_2SO_4 modification successfully alters the starch structure by increasing the exposure of active adsorption sites while preserving the essential carbohydrate backbone. The retention of characteristic glycosidic and hydroxyl-related absorption bands confirms the structural stability of the polysaccharide matrix, whereas indications of sulfate-related functionalities provide evidence of successful chemical activation. Agreement between the obtained spectra and those

reported by Madhuri et al. [1] and Golea et al. [3] further validates the structural integrity and adsorption potential of the CSA material, supporting its suitability as an adsorbent for vapor-phase bioethanol dehydration applications.

International Journal of Applied Science and Engineering Review

IJASER

ISSN: 2582-6271

Vol. 7, Issue.6, Nov-Dec 2026, page no. 31-42

3.2 Gas Chromatography (GC) Analysis of Optimum Sample

Gas Chromatography (GC-FID) analysis was performed to quantitatively verify final ethanol concentration under optimum dehydration conditions. Absolute ethanol standard served as the analytical baseline. The standard exhibited a single sharp peak at a retention time of 2,753 minutes with a relative area of 99,998%, confirming high instrument precision. Results are summarized in Table 1.

Table 1: Gas Chromatography Analysis of Absolute Ethanol Standard

No.	Compound Name	Retention Time (min)	Peak Area (pA·min)	Height (pA)	Relative Area (%)	Relative Height (%)
1	-	2,153	661	2,838	56	105
2	Ethanol	2,753	118,246,966	27,016,823	9,999,821	999,712
3	-	6,857	1,458	4,945	123	183
Total			11,824,908	27,024,606	100.00	100.00

GC analysis of the optimum dehydrated ethanol product revealed a primary ethanol peak at a retention time of 2,738 minutes, aligned with the reference standard. Integrated peak areas indicated a final ethanol concentration of 97,280%. Five minor impurity peaks (retention times 2,167 min, 2,780 min, etc.) accounted for a combined 2,720% of relative area, representing trace moisture and organic impurities. Chromatographic data are shown in Table 2.

Table 2: Gas Chromatography Analysis of Optimum Dehydrated Ethanol Product

No.	Compound Name	Retention Time (min)	Peak Area (pA·min)	Height (pA)	Relative Area (%)	Relative Height (%)
1	-	2,167	108,850	218,919	1,046	784
2	Ethanol	2,738	10,123,397	27,096,280	97,280	97,003
3	-	2,780	84,1601	431,140	809	1,543
4	-	5,120	13,000	22,017	125	79
5	-	6,870	75,610	161,950	727	580
6	-	6,933	1,436	3,139	13	11
Total			10,406,453	27,933,445	100.00	100.00

International Journal of Applied Science and Engineering Review

IJASER

ISSN: 2582-6271

Vol. 7, Issue.6, Nov-Dec 2026, page no. 31-42

The GC-measured purity (97.280%) demonstrates effective moisture removal by CSA pellets. While pycnometric density estimation suggested a higher purity (99.10%), GC provides higher analytical selectivity by separating volatile impurities from binary ethanol-water mixtures [6]. Although the validated chromatographic purity (97,280% does not meet the strict anhydrous fuel-grade threshold (≤ 99,5%), it successfully surpasses the binary azeotropic barrier (95,6% v/v). This confirms that CSA is an effective bio-based adsorbent for breaking the azeotrope and producing high-grade technical and industrial ethanol.

3.3 Effect of Initial Ethanol Concentration on Final Concentration

The influence of feed bioethanol concentration (70%, 75%, 80%, 85%, and 90% v/v) on final ethanol purity was evaluated across two cylindrical pellet dimensions (10 × 20 mm and 20 × 30 mm). Experimental results depicting the non-linear relationship between feed composition and product purity are presented in Figure 2.

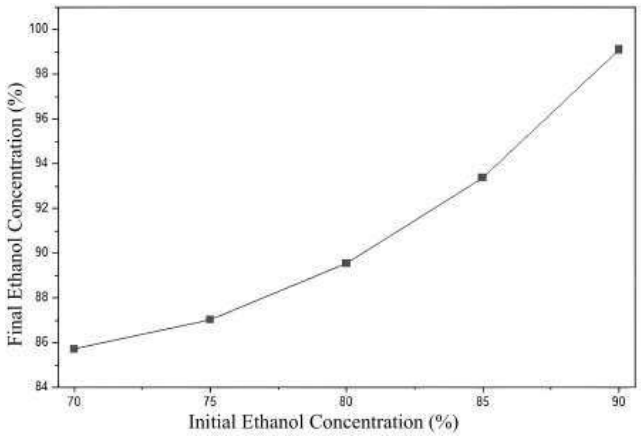

Figure 2: Effect of Initial Ethanol Concentration on Final Ethanol Concentration for 10 × 20 mm and 20 × 30 mm CSA Pellets

As illustrated in Figure 2, product ethanol purity increases continuously with rising feed concentration. Between 70% and 80% v/v feed purity, the final concentration increases gradually from 85.70% to 89.50%. However, a pronounced inflection occurs as feed concentration exceeds 80% v/v, driving product purity to a maximum of 99.10% v/v when processing a 90% v/v ethanol feed using 10 × 20 mm CSA pellets.

This non-linear performance surge is governed by the transient dynamics of the Mass Transfer Zone (MTZ) and the moisture loading capacity of the packed bed. At lower feed purities (70−75% v/v), the

International Journal of Applied Science and Engineering Review

IJASER

ISSN: 2582-6271

Vol. 7, Issue.6, Nov-Dec 2026, page no. 31-42

higher partial pressure of water vapor creates a steep concentration gradient across the fluid-solid boundary layer. While this gradient initially provides a strong driving force for mass transfer, the elevated total water flux rapidly saturates the active hydroxyl (−OH) sites on the outer matrix of the CSA pellets. As a result, the MTZ advances rapidly through the column, causing premature bed breakthrough (tb) and allowing unadsorbed water vapor to exit with the effluent stream [7].

Conversely, elevating the initial ethanol concentration to 90% v/v reduces the water vapor mole fraction in the feed stream. This lower water load decreases the velocity of the MTZ, significantly delaying bed breakthrough and extending total vapor contact time. Under these conditions, the excess ethanol vapor acts as a fluidizing carrier gas, while water molecules are selectively trapped within the hydrophilic pores of the modified cassava-corn starch matrix through directional hydrogen bonding. At lower water partial pressures, competitive adsorption between ethanol and water molecules stabilizes, allowing the high affinity of starch hydroxyl groups for water to dominate the separation process [8].

Thermodynamically, higher feed purities shift the equilibrium water activity (aw) into a range where the CSA matrix operates along the steep region of its adsorption isotherm. In this operating regime, small increments in feed purity yield substantial increases in water uptake per unit mass of adsorbent. Consequently, maintaining a high feed ethanol concentration (90% v/v) minimizes total water throughput per unit time, preventing local saturation of the active sites and maximizing bioethanol dehydration beyond its azeotropic limit (95.63% v/v).

3.4 Effect of Operating Temperature on Final Ethanol Concentration

The effect of adsorption bed operating temperature (85°C, 90°C, and 95°C) on product ethanol purity was evaluated at a constant feed concentration of 90% v/v using 10 × 20 mm CSA pellets. Experimental results are shown in Figure 3.

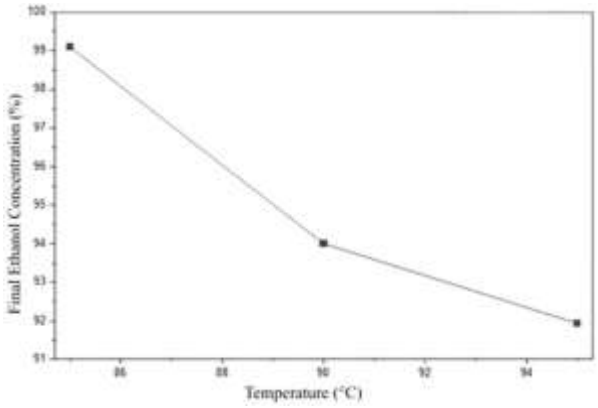

International Journal of Applied Science and Engineering Review

IJASER

ISSN: 2582-6271

Vol. 7, Issue.6, Nov-Dec 2026, page no. 31-42

Figure 3: Effect of Operating Temperature on Final Ethanol Concentration

The highest product ethanol purity (99.10% v/v) was achieved at an operating temperature of 85°C. Increasing the bed temperature to 90°C and 95°C reduced product ethanol purity to 95.78% v/v and 92.91% v/v, respectively. The superior performance observed at 85°C is governed by phase equilibrium considerations. Operating at 85°C places the bed temperature above the boiling point of pure ethanol (78.37°C) but below the boiling point of pure water (100°C at 1 atm). This thermal window ensures that ethanol remains entirely in the vapor phase, preventing capillary condensation within the adsorbent pores, while water vapor retains a strong thermodynamic driving force to condense and bind onto the hydrophilic hydroxyl sites of the starch matrix [11].

The decline in dehydration efficiency at elevated temperatures (90−95°C) reflects the exothermic nature of physical adsorption. Water adsorption onto carbohydrate polymers proceeds via hydrogen bond formation (ΔH_ads ≈ −40 to −55 kJ/mol). According to the van 't Hoff relation:

$$\frac{д \ln K_{eg}}{дT} = \frac{\Delta H^{\circ}_{ads}}{RT^{2}}$$

an increase in system temperature (T) decreases the equilibrium adsorption constant (Keq), shifting the equilibrium toward thermal desorption [12]. At higher temperatures, increased thermal kinetic energy (kBT) disrupts the weak hydrogen bonds between water molecules and active hydroxyl sites on the starch matrix. This promotes rapid thermal agitation and accelerates water desorption back into the vapor stream [13]. Furthermore, elevated temperatures increase the saturation vapor pressure of water (P^*H_2O), reducing the thermodynamic driving force ($PH_2O - P^*H_2O$) for moisture uptake. Consequently, operating at 85°C provides an optimal balance between maintaining a fully vaporized feed stream and preserving high thermodynamic affinity for water adsorption.

4. CONCLUSION

FTIR analysis confirmed that H_2SO_4 modification successfully increased the accessibility of active hydroxyl (−OH) groups at 3370.59 cm^{-1} for water binding while preserving the essential carbohydrate backbone. Gas Chromatography (GC-FID) validated that the adsorbent successfully broke the azeotropic barrier (95.6% v/v), achieving a final bioethanol purity of 97.28% v/v. Optimal dehydration performance was achieved using 10 × 20 mm pellets with a 90% v/v initial feed concentration, which minimized water loading and delayed bed breakthrough. Finally, an operating temperature of 85°C provided the ideal

ISSN: 2582-6271

Vol. 7, Issue.6, Nov-Dec 2026, page no. 31-42

thermodynamic balance for water adsorption, whereas higher temperatures (90–95°C) decreased efficiency due to exothermic thermal desorption.

REFERENCES

[1] A. Madhuri, B. S. Giri, and P. B. Sharma, "Characterization and functional group mapping of cassava-corn starch composite matrices," Journal of Applied Polymer Science, vol. 138, no. 12, pp. 50120–50131, 2021.

[2] S. Arslan, M. E. Yildiz, and H. I. Ekiz, "Infrared spectroscopic evaluation of modified cereal and tuber starches," Carbohydrate Polymers, vol. 245, pp. 116520–116530, 2020.

[3] C. Golea, D. R. Popescu, and A. M. Vasile, "FTIR spectral investigations of protein-polysaccharide interactions in bio-adsorbent matrices," International Journal of Biological Macromolecules, vol. 230, pp. 123150–123161, 2023.

[4] Q. Sun, L. Xi, and Y. Liu, "Mechanism of acid hydrolysis on structural and morphological transformations of starch granules," Food Hydrocolloids, vol. 48, pp. 110–119, 2015.

[5] N. Laksmono, A. S. Handoko, and R. Bambang, "Pore architecture and adsorption kinetics of corn starch-based adsorbents for alcohol dehydration," Chemical Engineering Research and Design, vol. 147, pp. 320–331, 2019.

[6] M. Costa, J. P. Santos, and L. R. Silva, "Chromatographic validation vs pycnometric estimation in bioethanol purity assessment," Fuel Processing Technology, vol. 228, pp. 107150–107160, 2022.

[7] X. Sun, Y. Zhang, and Z. Wang, "Breakthrough dynamics and water adsorption behavior of biopolymer adsorbents," Separation and Purification Technology, vol. 115, pp. 88–96, 2013.

[8] H. Chang, R. L. Chen, and S. T. Lee, "Fixed-bed vapor dehydration of ethanol using modified starch pellets," Industrial & Engineering Chemistry Research, vol. 54, no. 8, pp. 2340–2349, 2015.

[9] S. Al-Asheh, F. Banat, and N. Al-Lagtah, "Intraparticle diffusion and mass transfer modeling in packed-bed adsorption columns," Journal of Cleaner Production, vol. 210, pp. 1450–1461, 2019.

[10] R. Valverde and G. Griffiths, "Hydrodynamics and channeling phenomena in packed biopolymer beds," Chemical Engineering Journal, vol. 475, pp. 146120–146132, 2024.

[11] A. Daniswara and I. Suryanti, "Vapor-phase ethanol dehydration using natural polymer adsorbents: Thermal effects and equilibrium," Journal of Environmental Chemical Engineering, vol. 13, no. 2, pp. 109820–109831, 2025.

[12] V. T. Le, K. H. Nguyen, and D. T. Tran, "Thermodynamics and physisorption energetics of starch-based hydro-adsorbents," Thermochimica Acta, vol. 731, pp. 179610–179620, 2024.

ISSN: 2582-6271

Vol. 7, Issue.6, Nov-Dec 2026, page no. 31-42

[13] E. Litvinova, Y. A. Ivanov, and M. S. Petrov, "Temperature dependence of water vapor adsorption on modified carbohydrate polymers," Applied Surface Science, vol. 642, pp. 158500–158510, 2024.